Journal of Polymers and the Environment (2020) 28:2599–2615
https://doi.org/10.1007/s10924-020-01793-w

ORIGINAL PAPER

The Influence of Vanillin Acrylate Derivative on the Phase Separation Temperature of Environmental Photo-Cross-Linked N-isopropylacrylamide Copolymer and Hydrogel Thin Films

Momen S. A. Abdelaty[1]

Published online: 24 June 2020

Abstract

The present study emphasizes the fabrication of thermal and pH-responsive photo-cross-linked polymers and hydrogel thin films. N-isopropylacrylamide was used as a thermal responsive monomer, while a new pH-responsive monomer was synthesized based on vanillin 2-((dimethylamino)methyl)-4-formyl-6-methoxyphenyl acrylate (DMAMVA). The photo-cross-linker (DMIA) and adhesion promotor (DMITAAc) have been prepared. All compounds were investigated by 1H NMR, 13C NMR, and FTIR. Terpolymers of 10, 15, and 20 mol% DMAMVA and 10 mol% of DMIA with N-isopropylacrylamide were fabricated. The chemical structures were investigated, and the molecular weights were determined by gel permeation chromatography GPC. Moreover, the glass transition temperatures were also recorded by differential scanning calorimeter DSC. The lower critical solution temperatures of polymers were determined by turbidity tests using UV–Vis spectroscopy. The polymer solution of 20 mol% sample was spin-coated over the gold to form hydrogel thin film within photo-cross-linking by the UV lamp. The film thickness was determined by the SPR-OW technique using Kretschmann configuration. The swelling was recorded and the transition temperature of hydrogel was determined as the change in volume degree of swelling and refractive index with the change in temperature. The dual responsive functional photo-cross-linked polymers and hydrogel thin films have significant importance in the grafting of some biological molecules.

Graphic Abstract

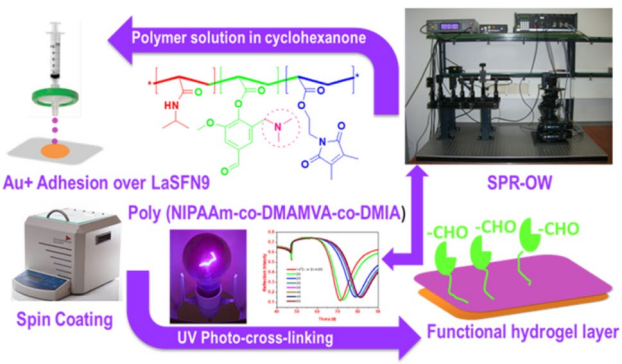

Keywords Phase separation · Environmental polymer · Photo-cross-linked polymer · Vanillin · Hydrogel thin films

Introduction

First and foremost, we should discuss the meaning of environmental material; it is a material that can change their chemical or physical behavior by changing the surrounding

✉ Momen S. A. Abdelaty
abdelatymomen@yahoo.com

[1] Polymer Lap, Chemistry Department, Faculty of Science (Assiut), Al-Azhar University, Assiut 71524, Egypt

environment. These polymeric materials are famous for stimuli, responsive, stimuli-responsive, smart, and intelligent [1–6]. The scientists have revealed many kinds of responsiveness like thermal, pH, ionic, magnetic, dielectric, and mechanical responsiveness [7–11]. A hydrogel is a hydrophilic 3D network that can absorb a large amount of water [12]. Recently, environmental hydrogel or stimuli-responsive hydrogel has been widely used; they are capable to change their dimension as swell and collapse according to their environmental responsiveness [13]. Thermo-responsive and the pH-responsive hydrogel are the most popular, due to their widely numerous applications [14–20]. Firstly, a thermo-responsive hydrogel is a kind of environmental hydrogel can change their morphological feature as well as their physical properties as soon the surrounding temperature has been changed [21]. N-isopropylacrylamide polymer hydrogel is the most intensive material was used for that purpose; the phase separation and the lower critical solution temperature of PNIPAAm hydrogel (LCST) have been recorded at 32℃; before this point, the hydrophilic groups have dominated and hydrogel absorbs water and therefore swell. On the other hand, by raising the temperature above the LCST the hydrophobic groups have a great effect and the hydrogel pores release water and start to collapse step by step with raising the temperature [22–24]. Several applications of PNIPAAm hydrogel were used in biosensor and bio-actuator [25–29]. A pH-responsive hydrogel is a polyelectrolyte that can change its shape (swelling/shrinking) by changes in the pH of the ambient environment [30–33]. It was classified into two kinds e.g. anionic and cationic according to the ionization of functional pendant group in the polymer main chain, meanwhile, the ionization is responsible for the formation of electrical charge; meanwhile, the electrostatic repulsion between hydrogel charges and the pH solution has been generated and responsible for the hydrogel deformation [34]. Polycarboxylic acid, like polyacrylic acid PAA, has been used in the formation of the polyanionic hydrogel in an alkaline pH environment, while, the polyamine acted as polycationic hydrogel in acidic pH environment like poly (N, N-dimethylaminoethylmethacrylate) PDEAEMA [35, 36]. The last decades have witnessed many applications of the pH-responsive hydrogel in bio-separation, drug delivery, biosensor, and bio-actautor [33, 37–43]. Moreover, the formation of dual responsive hydrogel has been done by the copolymerization of different thermo-responsive with pH-responsive. The copolymerization of PNIPAAm with PAA and PDEAEMA has been widely used in the formation of thermos-pH dual responsive hydrogel for the formation of the biocompatible vessel for targeting biomolecules [44–50]. The additional functional groups in the hydrogel backbone improving the hydrogel properties e.g. grafting and branching that can be used in the bio-separation process [51–54]. Vanillin plays an avital role in the formation of functional monomers and polymers due to the presence of hydroxyl and aldehyde group; furthermore, it has bioactivity properties e.g. anti-carcinogenic activities, anti-mutagenic, and anti-microbial [55–57]. New studies have been developed sustainable and renewable environmental polymers and hydrogel for biodegradable material [58, 59]. In the current and past decade, many scientists have been focused on the preparation of hydrogel thin films. Surface plasmon resonance spectroscopy with optical waveguide spectroscopy (SPR/OW) has been used as a new technique for thickness measurement and determination of LCST of thermos-responsive hydrogel depending on the change of volume degree of swelling or refractive indexes with temperature as well as thermos-pH dual responsive hydrogel [60–65]. Eventually, this work describes the preparation of new pH-responsive monomer that further used for the preparation of dual responsive polymers and their photo-cross-linked hydrogel thin film over gold; the study of phase separation of the polymer solution, as well as hydrogel thin film, has our attention.

Experimental

Materials

Acryloyl chloride (99%, Merck, Germany), di-tert-butyl-dicarbonate ($(boc)_2O$) (98%, Acrōs, Germany) ethanolamine (98%, Fluka, Germany), dimethyl maleic anhydride (98%, Aldrich, Germany), allyl amine (98%, Merck), dimethylamine (98%, Aldrich, Germany), N-isopropylacrylamide (NIPAAm) (97%, Fluke, Germany) was recrystallized from distilled n-hexane (n-hexane stirred overnight in $MgSO_4$ then distilled). Vanillin (99%, Aldrich, Germany), 2, 2′-azobis (isobutyronitrile) (AIBN) (96%, Acrōs, Germany) was recrystallized from methanol, thioxanthone (Acrōs), triethylamine (Merck), dichloromethane (DCM), sodium carbonate (Grüssing), magnesium sulphate (Merck), dioxane, tetrahydrofuran (THF), cyclohexanone (95%, Fluke, Germany) was purified by distillation after drying overnight in magnesium sulphate, diethylether were distilled over potassium hydroxide, and gold (Au, 99.999%, Aldrich Germany). Other chemicals were used as purchased.

Instrumentations

The functional groups for each monomer and polymer were detected by Vertex 70 Fourier transform infrared instrument FT-IR, the samples were dried and milled with KBr and the functional absorption was recorded. For 1H and 13C Bruker, AV 500 spectrometer in $CDCl_3$ or d^6 DMSO as solvent was used; it was 500 MHz and 125 MHz for 1H and 13C NMR respectively.

Molecular weights (Mn, Mw) and the dispersity (*Đ*) were recorded by Size exclusion chromatography (SEC) in tetrahydrofuran (THF) as eluent (containing 0.1 vol% triethylamine) with a flow rate of 0.75 mL/min at 30 ℃. The concentrations of samples were (16 mg/mL), automatic sample injection. PSS-SDV with 5 µm gel Columns was used, and polystyrene was used as standard.

The phase separation and the lower critical solution temperature (*Tc*) has been determined by UV–Vis spectrometer (Perkin Elmer Lambda 45); it has fixed by metal covet stand that allowed water cycle input and output in heating and cooling by connecting to a thermocouple to adjust the temperature, the temperature rate was taken as 2 °C/min over the range from 5 to 80 ℃; The polymer solution was 1 wt% in deionized water or pH buffer solution.

The glass transition temperature (T_g) of solid polymers was recorded by Perkin Elmer Differential Scanning Calorimeter Pyris 1 in heating and cooling rate of 5 ℃/min.

The gold film has been deposited by physical vapor deposition (PVD) (tectra GmbH). G3P-8 Spin Coat was used to perform polymer thin film. UV Hg-lamp (OSRAM, 100W) fixed with an optical lens and a mirror has been used for photo-cross-linking and formation of the gel. The swelling properties and hydrogel thin films were recorded by Surface plasmon resonance (SPR) added to optical waveguide (OWS), (Restech) is used to perform this process. He–Ne laser beam with a wavelength of 632.8 nm was used to excite SPs in Kretschmann configuration.

Experiments

Synthesis of Monomer

Synthesis of 2-((Dimethylamino)methyl)-4-Formyl-6-Methoxyphenyl Acrylate (2) (DMAMVA) *Step 1: Synthesis of 3-((dimethylamino)methyl)-4-hydroxy-5-methoxy-benzaldehyde* (***1***)

Vanillin (4-hydroxy-3-methoxy benzaldehyde) 16 g (0.1 mol), formaldehyde 16 g (0.53 mol), and 16 g (0.36 mol) dimethylamine all were dissolved in 250 mL ethanol in 500 mL round bottom flask fixed with a water condenser and water trap; they allowed refluxing for 4 h in an oil bath. After two hours the orange precipitate has appeared. The flask was taken off and then allowed to cool at the room temperature and filtered to collect the product. The solvent was also reduced under pressure to collect the rest of the product. Yield 97%, orange solid, m.p. = 140 ℃

^{1}H NMR (500 MHz, $CDCl_3$): δ (ppm) = 2.37 (s, 6 H, i-N(CH_3)2), 3.75 (s, 2 H, h-Ar-NCH_2), 3.93 (s, 3 H, j-OCH_3), 6.39 (br, 1 H, k-OH), 7.15 (d, 1 H, ^{4}J = 1.8 Hz, d-Ar-CH), 7.33 (d, 1 H, ^{4}J = 1.8 Hz, c-Ar-CH), 9.76 (s, 1 H, a-CHO).

^{13}C-NMR (125 MHz, $CDCl_3$): δ (ppm) = 44.32 (2 C, i-NCH_3), 56.01 (1 C, h-NCH_2), 62.21 (1 C, j-OCH_3), 109.97 (1 C, d-Ar-CH), 123.70 (1 C, c-Ar-CH), 125.21 (1 C, g-Ar-C), 128.09 (1 C, b-Ar-C), 148.68 (1 C, f-Ar-C), 154.54 (1 C, e-Ar-C), 190.67 (1 C, a-CHO).

IR (KBr): ν (cm^{-1}) = 3300 (s) NH, OH, 2989 (s) (CH_2, CH_3), 1744 (s) (C=O), 1646 (s) (C=C), 816–837 (m) (Ar-CH).

Step 2: Synthesis of 2-((dimethylamino)methyl)-4-formyl-6-methoxyphenyl acrylate (***2***) (*DMAMVA*).

13.5 g (0.062 mol) 3-((dimethylamino)methyl)-4-hydroxy-5-methoxy-benzaldehyde (1) and 12 g (0.3 mol) sodium hydroxide all were dissolved in 200 mL dry dichloromethane in 500 mL three-neck flask fixed with a balloon of nitrogen gas, dropping funnel and connected to water condenser. The mixture was stirred strongly in an inert atmosphere. After about 30 min they allowed to cool to 0–5 ℃ and 5.6 g (0.062 mol) acryloyl chloride in 25 mL dry CH_2CL_2 was slowly dropped to the mixture using the dropping funnel, the yellowish suspension started appeared and the mixture was stirred at 5 °C for 1 h, and then allowed to stir at RT for 6 h. the reaction was finished and the precipitate was then filtered and the solvent was evaporated by vacuum rotatory. It has been purified by dissolving in methylene dichloride and washing three times with DI water, one time with 0.1 M sodium bicarbonate, and rewashed with DI water. After drying over magnesium sulfate overnight and filtered, then the solvent was removed to collect the final product. Yield 75%, orange viscous liquid.

^{1}H NMR (500 MHz, $CDCl_3$): δ (ppm) = 2.19 (s, 6 H, i-2CH_3), 3.37 (s, 2 H, h-NCH_2), 3.84 (s, 3 H, h-OCH_3), 6.03 (dd, ^{2}J = 1.1 Hz, ^{3}J = 10.5 Hz,1 H, m1 = CH_2), 6.34 (dd, ^{3}J = 10.5 Hz, ^{3}J = 17.3 Hz, 1 H, l = CH), 6.64 (dd, ^{2}J = 1.1 Hz, ^{3}J = 17.3 Hz, m2 = CH_2), 7.37 (d, 1 H, ^{4}J = 1.7 Hz, d-Ar-CH, 7.34 (d, 1 H, ^{4}J = 1.7 Hz, c-Ar-CH), 9.91 (s,1 H, a-CHO).

^{13}C-NMR (125 MHz, $CDCl_3$): δ (ppm) = 45.42 (2 C, i-2CH_3), 55.72 (1 C, h-NCH_2), 62.41 (1 C, j-OCH_3), 108.75 (1 C, d-Ar-CH), 122.37 (1 C, c-Ar-CH), 126.25 (1 C, l = CH), 127.30 (1 C, g-Ar-C), 132.22 (1 C, 5-Ar-C), 134.39 (1 C, m = CH_2), 143.50 (1 C, b-Ar-C), 152.51 (1 C, e-Ar-C), 162.81 (1 C, k-COO), 191.64 (1 C, a-CHO).

IR (KBr): ν (cm^{-1}) = 2939(s) (CH_2, CH_3), 1718 (s) (C=O), 1665 (s) (C=O), 1615(s) (C=C), 874–826 (m) (Ar-CH).

Synthesis of Dimethylmaleimidoacrylate (DMIA) Photo-Cross-Linker

Step 1: Synthesis of dimethylmaleimido ethanol or 1-(2-hydroxyethyl)-3,4-dimethyl-1H-pyrrole-2,5-dione (***3***).

In a 500 ml round bottom flask fitted with a water trap, 12.623 g (0.206 mol) of 2-aminoethaol was added to the stirred solution of 12.611 g (0.1 mol) dimethylmaleic anhydride in 300 mL toluene. The mixture was refluxed at about 135 °C in an oil bath for 4 h. The solution was cooled to RT. The solvent was evaporated under reduced pressure. The product was purified by TLC using 1:1 n-hexane: ethyl acetate as eluent and silica (R_f = 0.32), 72% (lit.: 74%), colorless, crystals.

^{1}H NMR (500 MHz, $CDCl_3$): δ (ppm) = 1.97 (s, 6H, a-CH_3), 2.20 (br.; 1H, f-OH), 3.70 (t, 2H, ^{3}J = 5.85 Hz, d-CH_2), 3.77 (m, 2H, ^{3}J = 4.89 f-CH_2).

^{13}C-NMR (125 MHz, $CDCl_3$): δ (ppm) = 8.70 (2C, a-CH_3), 40.91 (1C, d-CH_2), 61.38 (1C, e-CH_2), 137.42 (2C, b-C=C), 172.82 (2C, c-C=O).

IR (KBr): ν (cm^{-1}): 3500 (m) (OH), 3080–2945 (s) (CH_2, CH_3), 1765 (C=O), 1705(s) (C=C), 1005 (s) (OH).

Step 2: Synthesis dimethylmaleimidoacrylate (DMIA) (***4***) [66].

In two neck flask fitted with nitrogen balloon. 5.57 g (0.032 mol) of **(3)** in 100 mL dry CH_2Cl_2 was stirred and, 6.70 g (0.066 mol) of TEA was added. The mixture was allowed to cool to 0–5 ℃ in an ice bath. 3.33 g (0.0368 mol) of acryloyl chloride was added dropwise. The yellowish suspension was stirred at 5 ℃ for 1 h and then allowed to stir at RT overnight. The suspension was filtered and, the filtrate was evaporated under reduced pressure to remove the solvent. The product was purified by TLC in 1:2 n-hexane to ethyl acetate R_f = 0.45, 97%. (lit.: 98%) [66], colorless viscous liquid.

^{1}H NMR (500 MHz, $CDCl_3$): δ(ppm) = 1.95 (s, 6H, a-CH_3), 3.78 (t, 2H, ^{3}J = 5.45 Hz, d-CH_2), 4.26 (t, 2H, ^{3}J = 5.33 Hz, e-CH_2), 5.82 (dd, ^{2}J = 1.4 Hz, ^{3}J = 10.3 Hz, h1-CH), 6.07(dd, ^{3}J = 10.4 Hz, ^{3}J = 17.35 Hz, 1 H, g-CH), 6.37 (dd, ^{2}J = 1.4 Hz, ^{3}J = 17.3 Hz, h2-CH).

^{13}C-NMR (125 MHz, $CDCl_3$): δ (ppm) = 8.66 (2C, a-CH_3), 36.81 (1C, d-CH_2), 61.79 (1C, e-CH_2), 128.01 (1C, g-CH), 131.28 (1C, h-CH_2), 137.36 (2C, b-C=C), 165.76 (1C, f-C=O), 172.45 (2C, c-C=O).

IR (KBr): ν (cm^{-1}): 3080–2945 (s) (CH2, CH_3), 1670–1730 (s) (C=O), 1640 (s) (C=C).

Synthesis of Adhesion Promotor

Preparation of Thioacetic Acid 3-(3,4-Dimethyl-2,5-Dioxo-2,5-Dihydro-pyrrol-yl)-propyl Ester (DMITAc) Adhesion Promoter

The DMITAc was prepared according to the literature [67].

Step 1: Synthesis of 1-allyl-3,4-dimethyl-pyrrol-2,5-dione (5).

A mixture of 5.71 g (0.1 mol) of allylamine and 6.305 g (0.05 mol) of dimethyl maleic anhydride was dissolved in 200 mL toluene in 250 mL round-bottomed flask fitted with a water trap to collect water. It has been refluxed under stirring in an oil bath at about 130 ℃ for 4 h. The reaction has been finished and 1.5 mL of water was collected in the water trap. After cooling at room temperature the mixture was filtered and then the solvent was removed under reduced pressure. The crude product was purified by TLC by dissolving in 4:1 n-hexane to ethyl acetate as eluent and using silica gel as stationary phase, R_f = 0.5, white, slurrish solid, 70% (lit.: 75%) [67].

1H NMR (500 MHz, $CDCl_3$): δ(ppm) = 1.96 (s, 6H, a-2CH3), 4.08 (tt, 2H, 2J = 1.5 Hz, 3J = 5.6 Hz, d-CH2), 5.14 (ddd, 1H, 2J = 1.2 Hz, 3J = 27.1 Hz, 3J = 10.2 Hz, 3J = 17.1 Hz, 4J = 1.1 Hz, g 1,2-CH)), 5.80 (ddd, 1H, 3J = 27.3, 3J = 17.2 Hz, 3J = 6.97 Hz, 3J = 5.7 Hz, f-CH).

13C-NMR (125 MHz, $CDCl_3$): δ(ppm) = 8.64 (2C, a-CH3), 39.97 (1C, d-CH2), 117.25 (1C, f-CH2), 132.04 (1C, b-CH), 137.32 (2C, g-C=C), 171.73 (1C, c-C=O).

IR (KBr): ν (cm^{-1}): 2960 (s) (CH-Aliphatic), 1720–1740 (s) (C=C), (C=O).

Step 2: Synthesis of thioacetic acid 3-(3, 4-dimethyl-2,5-dioxo-2,5-dihydro-pyrrol-yl)-propyl ester (DMITAc) (6).

In 50 mL round bottom flask with reflux condenser, 3.454 g (0.045 mol) of thioacetic acid was added to stir solution of 5 g (0.03 mol) 1-allyl-3,4-dimethyl-pyrrol-2,5-dione (5), and 0.294 g (1.79 mmol) AIBN in 30 mL $CHCl_3$. The mixture was refluxed at 80 ℃ for 5 h in an oil bath. The reaction was finished and the mixture was allowed to cool at room temperature. 50 mL of 1 M sodium bicarbonate was added. The aqueous solution was extracted two times using 60 mL diethyl ether, followed by the addition of sodium chloride till saturation, dried with MgSO4 overnight. The product was purified by TLC using 4:1 n-hexane to ethyl acetate as eluent and silica gel as stationary phase R_f = 0.32, followed by vacuum distillation for extra purification. Colorless viscous liquid, 88% (lit.: 84%) [67].

^{1}H NMR (500 MHz, $CDCl_3$): δ (ppm) = 1.83 (p, 2H, ^{3}J = 6.9, f-CH_2), 1.93 (s, 6H, a-CH_3), 2.28 (s, 3H, i-CH_3)), 2.79 (t, 2H, ^{3}J = 7.3, g-CH), 3.50(t, 2H, ^{3}J = 6.9, d-CH).

^{13}C-NMR (125 MHz, $CDCl_3$): δ (ppm) = 8.6 (2C, a-CH3), 26.28 (1C, f-CH2), 28.70 (1C, g-CH_2), 30.51, (1C, i-CH_3),

36.72 (1C, d-CH_2), 137.17 (2C, b-C=C), 172.07 (1C, c-C=O), 195.33 (1C, h-C=O).

IR (KBr): ν (cm^{-1}): 2962 (s) (CH-Aliphatic), 1741–1723 (s) (3-C=O), (2-C=C), 1705 (7-C=O).

Synthesis of Photo-Cross-Liked Terpolymer

In 100 mL round bottom flask closed with a rubber stopper. A mixture of 0.296 g 5 mol% of dimethylmaleimidoacrylate, photo-cross-linker (DMIA) (4) was added to 0.679, 0.887 and 1.183 g, 10, 15 and 20 mol% respectively of 2-((ditert-butylamino)methyl)-4-formyl-6-methoxyphenyl acrylate (DMAMVA) (3) and 3.00 g (0.0265 mol) N-isopropylacrylamide (NIPAAm) and 2,2′-azobis(isobutyronitrile) (AIBN) were dissolved in 60 mL pure 1,4-dioxane. The mixture was purged in nitrogen for 20 min. and then heated with stirring in an oil bath at 70–75 ℃ for 8 h. The polymerization was terminated by cooling firstly at room temperature and then freeze overnight in the refrigerator. The polymeric material has been extracted by precipitation in diethyl ether at – 40 ℃. Further, it was dissolved in THF, and re-precipitated in diethyl ether to remove all unreacted monomers and impurities.

^{1}H NMR (500 MHz, $CDCl_3$): δ(ppm) = 0.92–1.28(m, 6H, m-CH3), 1.35–1.70(m, 6H, h, f-CH_2), 1.72–1.83 (m, 6H, a-CH3), 1.83–2.27 (m, 3H, e,g,i-CH), 2.35–2.98 (m, 4H, b,c-CH_2), 3.56–3.70 (m, 3H, p-CH3), 3.74–4.13(m, 1H, l-CH), 6.93–7.84 (m, 3H, k-NH, n–CH-Ar), 7.62–7.82 (m, 1H, 3-CH-Ar.), 9.92–10.03 (m, 1H, o-CHO).

IR (KBr): ν (cm-1): 3200–3500 (s) (NH, OH), 3095–2984(s) (CH-Aliphatic), 1763(s) (C=O, carbonyl), 1713(s) (C=O, aldehyde), 1607(s) (C=C), 1103 (s) (O-CH3), 805–857 (m) (CH-Aromatic).

The Formation of Hydrogel Thin Films has been Achieved in Five Steps Using Four Techniques and Instruments

1. Gold was deposited over LaSFN9 glass slides with a 45 nm gold film using physical vapour deposition (PVD) (tectra GmbH). High vacuum coating system for applying thin layers the coating chamber of the system is made of stainless steel and has the dimensions 300 mm, height 400 mm. The device offers the options for thermal and/or electron beam evaporation of the film-forming substances. The targets can be heated or cooled to improve the layer properties. The growth of the layers is recorded in situ using a quartz microbalance.
2. Au- substrate slide was immersed 24 h in DMITAc to form adhesion promoter about 5 nm thin film over Au.
3. The polymer was dissolved in cyclohexanone in 7.5 wt% and G3P-8 Spin Coat was used to perform polymer thin film. The conditions were 250 rpm for 30 s and 2000 rpm for 140 s.
4. UV Hg-lamp (OSRAM, 100 W) fixed with an optical lens and a mirror has been used for photo-cross-linking and formation of the gel.
5. The swelling properties and hydrogel thin films were recorded by Surface plasmon resonance (SPR) added to optical waveguide (OWS), (Restech) is used to perform this process. He–Ne laser beam with a wavelength of 632.8 nm was used to excite SPs in Kretschmann configuration. The swelling properties of hydrogel with the response to temperature and pH were measured as follows; 3–4 mL of distilled water or pH solution has been handle injected to the SPR cell (SPR cell consists of a sample holder, LaSFN9 glass with a gold coating, a prism. The temperature was controlled by a Peltier element in addition to a thermocouple of 0.1 ℃ accuracy has been also used to measure the temperature inside the cell.

Result Analysis and Discussion

Synthesis of Monomer, Photo-Cross-Linker, Adhesion Promotor and Polymers

Syntheses of new monomer, photo-cross-linker, and adhesion promotor have been performed to serve our eventual goal for preparation environmental functional photo-cross-linked polymers and hydrogel thin films as well. Firstly, the new monomer based on vanillin was synthesized to act as a pH-responsive monomer; it was synthesized in two steps reaction. The first step was described in Scheme 1 as the reaction of vanillin with both formaldehyde and dimethylamine in basic or in a neutral condition. The reaction proceeded according to Mannich reaction mechanism. The product was 3-((dimethylamino)methyl)-4-hydroxy-5-methoxy-benzaldehyde (1) and demonstrated logic results with the chemical structure; the 1H NMR and 13C in Fig. 1 showed the presence of dimethyl group –(CH_3)$_2$ at δ = 2.73 ppm and methylene –CH_2N– at δ = 3.75 ppm that corresponding to 44.5 and 56.01 ppm 13C NMR. The next step for the preparation of the final product was achieved by the reaction of compound (**1**) with the acryloyl chloride in strong basic condition and in an inert atmosphere as shown in Scheme 1. The chemical structure was elucidated by the 1H NMR and 13C in Fig. 2; the vinyl group has been appeared in the region from 6.03 to 6.64 ppm and 126.25 and 134.39 ppm for 13C, the stability of aldehyde group has also been detected at 9.91 and 191.64 ppm for each 1H and 13C. For compounds 1 and 2, the FTIR has also been used to investigate the presence of functional groups, and it was successful to detect the aldehyde group -CHO as a stretched peak at 1718 cm^{-1} in addition to vinyl group C=C at 1665 cm^{-1}.

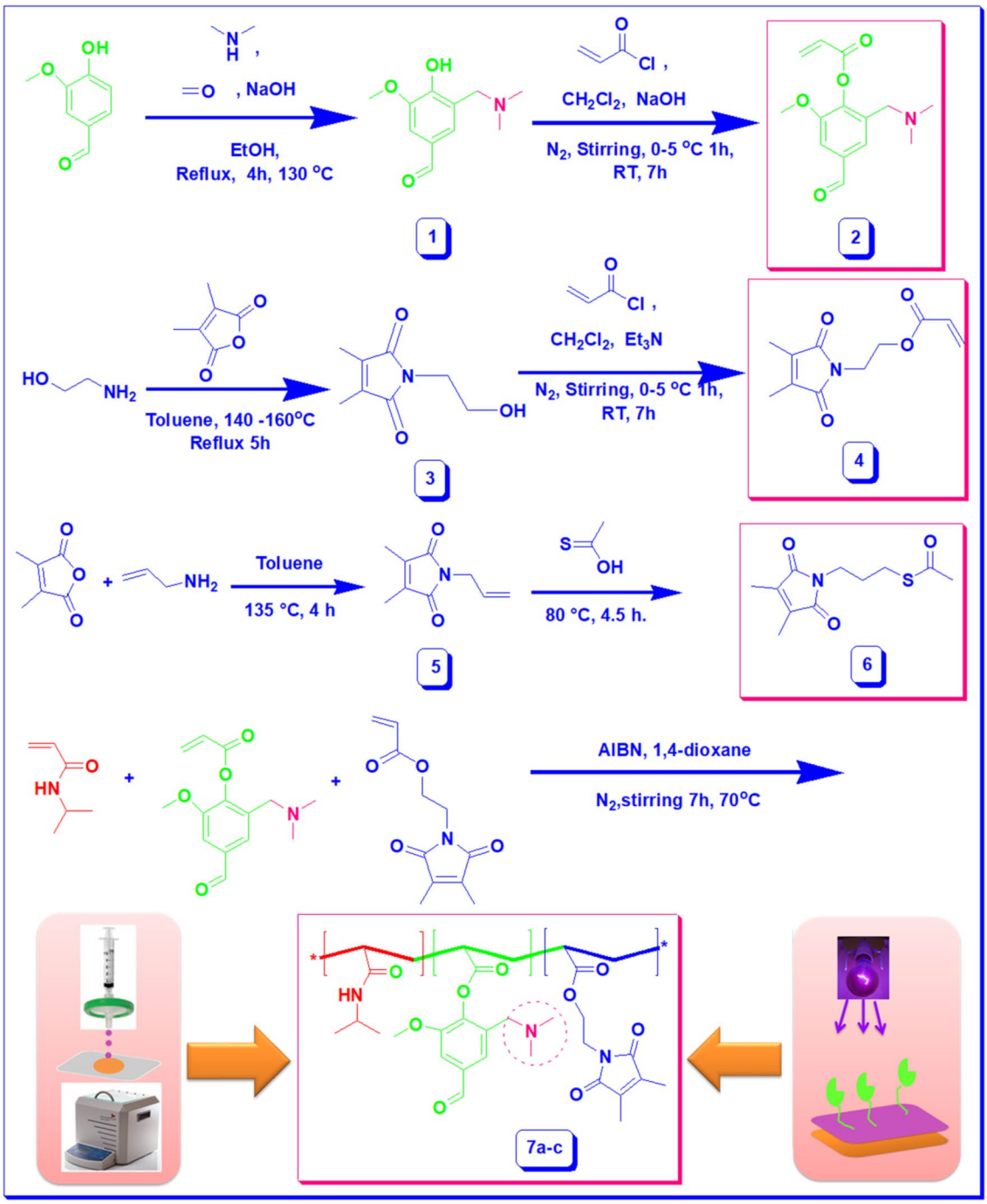

Scheme 1 Synthesis of DMAMVA monomer, photo-cross-linker, adhesion promotor, and polymers

The acrylate photo-cross-linker (DMIA) (4) was synthesized in a two-step process as outlined in Scheme 1. The first step in the synthesis of DMIA involved a condensation reaction between dimethyl maleic anhydride and ethanolamine with the subsequent removal of water as a by-product. The resulting colorless crystalline solid (3) was reacted with acryloyl chloride in the presence of triethylamine as base catalysis and dry dichloromethane and finally, lead to the formation of (4) the product in high yield (97%). Figures 3 and 4 show the 1H NMR of compounds 3, 4. The adhesion promoter for gold was synthesized for the covalent attachment of a thin hydrogel layer to the substrates. The active group on the surface is responsible for the chemisorption on the substrate. The molecular surface interactions are covalent Au–S bonds. The adhesion promoter for gold (DMITAc) (**6**) was

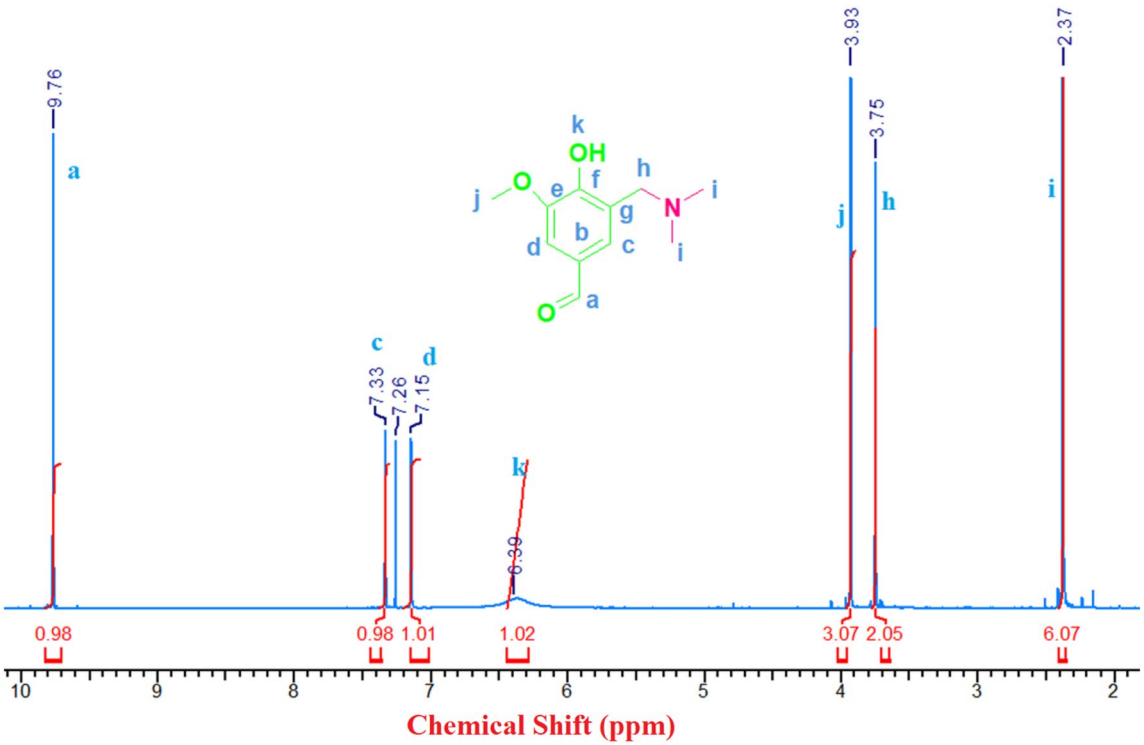

Fig. 1 1H NMR spectrum ($CDCl_3$) of 3-((dimethylamino)methyl)-4-hydroxy-5-methoxy-benzaldehyde (DMAMV) (**1**)

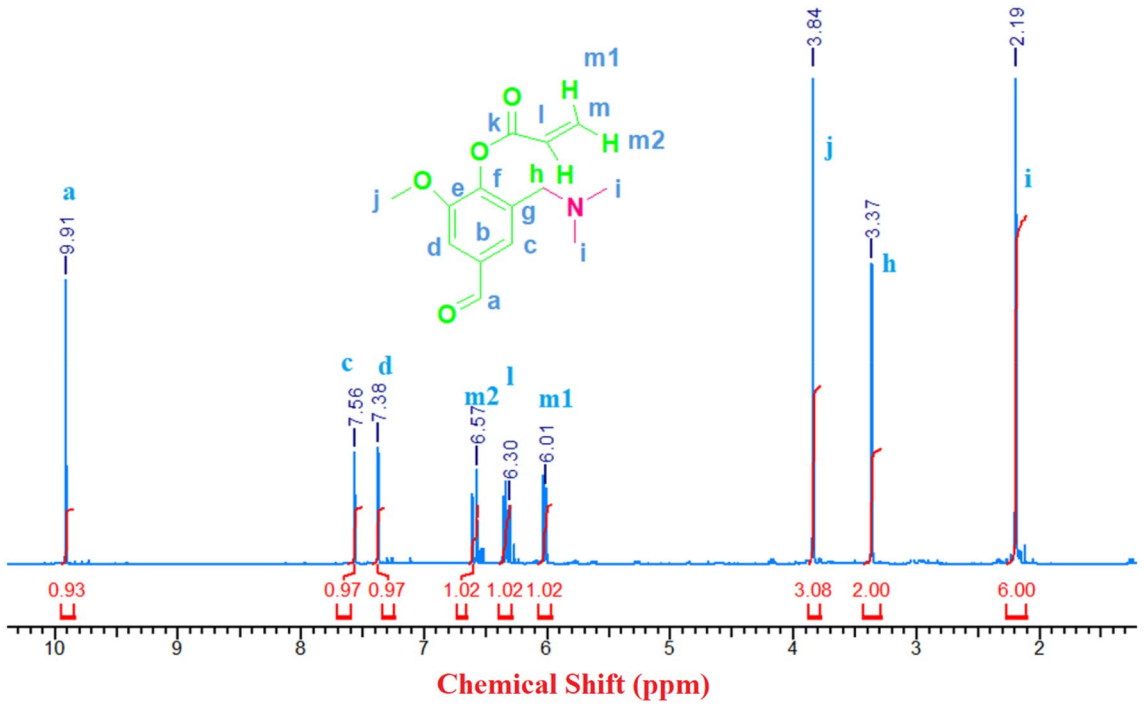

Fig. 2 1H NMR spectrum ($CDCl_3$) of 2-((dimethylamino)methyl)-4-formyl-6-methoxyphenyl acrylate (DMAMVA) (**2**)

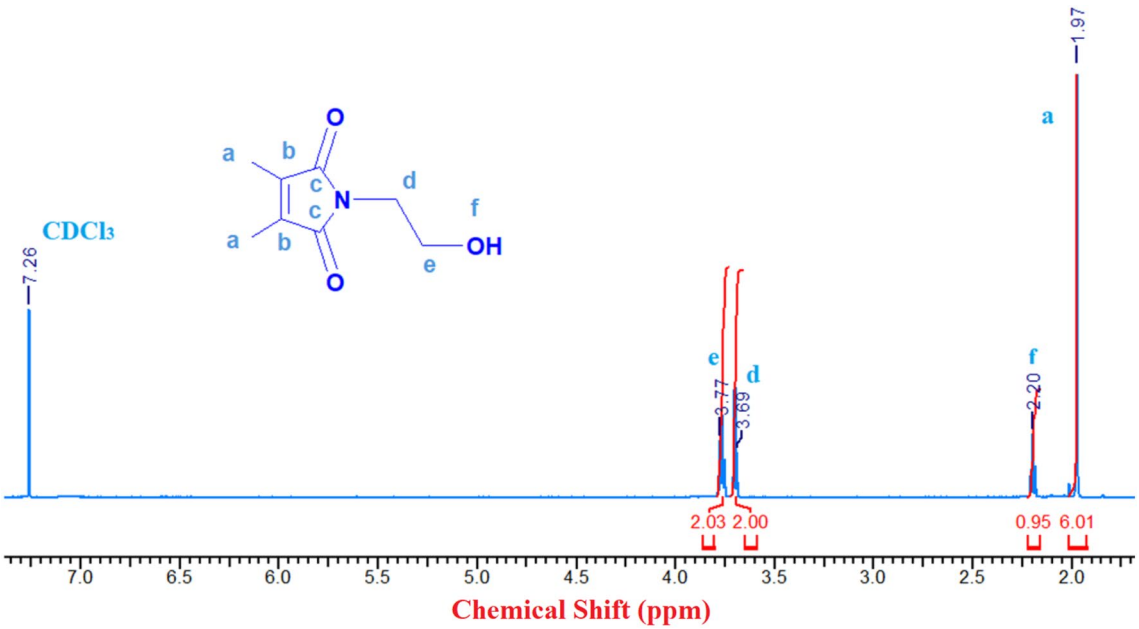

Fig. 3 1H NMR spectrum ($CDCl_3$) of 1-(2-hydroxyethyl)-3,4-dimethyl-1H-pyrrole-2,5-dione (**3**)

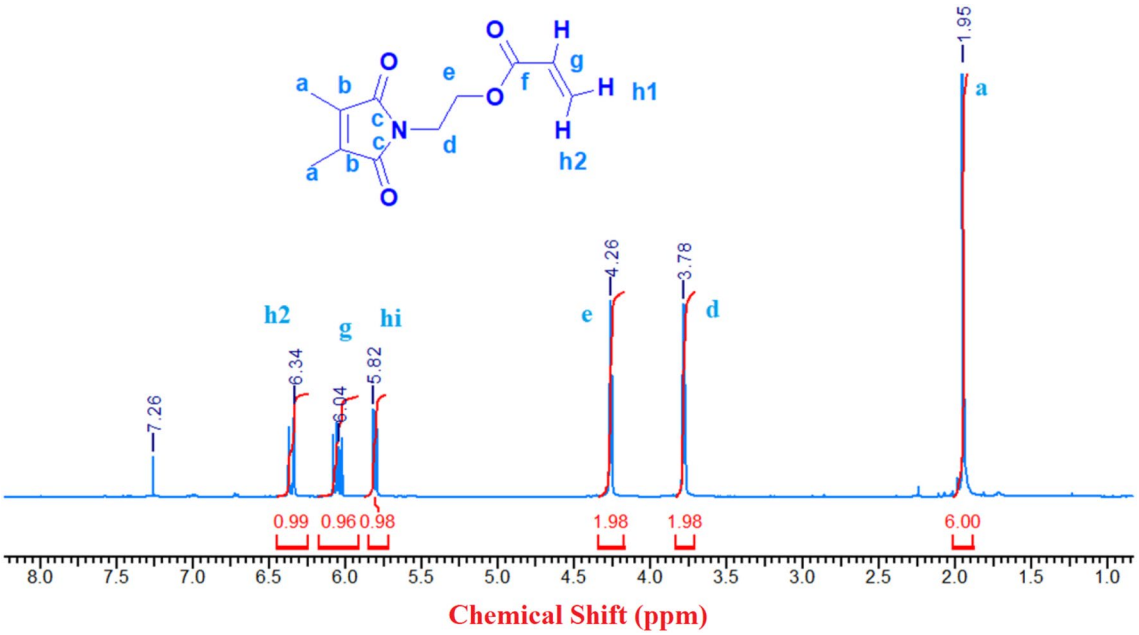

Fig. 4 1H NMR spectrum ($CDCl_3$) of dimethylmaleimidoacrylate (DMIA) (**4**)

synthesized in a two-step process as shown in Scheme 1. The first step involved the reaction of allylamine with dimethyl maleic anhydride and the removal of water as a by-product. In the second step, compound (**5**) was reacted with thioacetic acid in the presence of AIBN to yield the product (**6**). It was investigated by 1H NMR and 13C NMR and FTIR as shown in Figs. 5, 6, and 7.

Here, we synthesized a series of photo-cross-linked functional polymers in different mole ratios DMAMVA. Random free radical polymerization was used to synthesize polymers **7a–c**. The 1HNMR was performed to estimate the actual amount of DMIA and DMAMVA in the polymer chain. Three kinds of protons integrations the integration ($2CH_3$) of DMIA at 1.83–2.27 ppm, NIPAAm

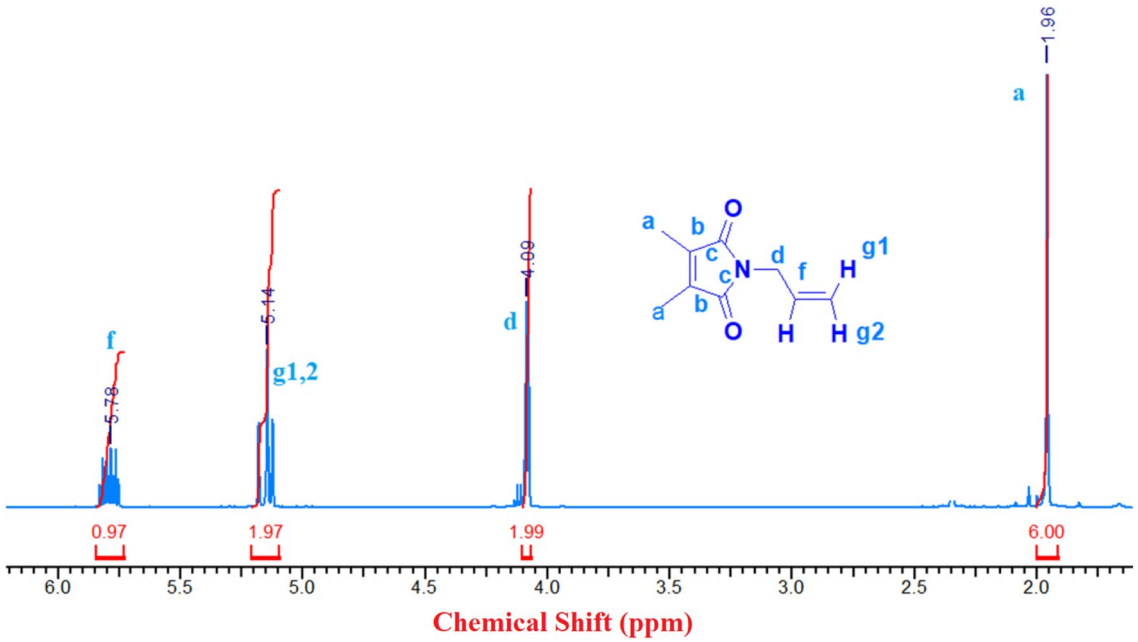

Fig. 5 1H NMR spectrum ($CDCl_3$) of 1-allyl-3,4-dimethyl-pyrrol-2,5-dione (**5**)

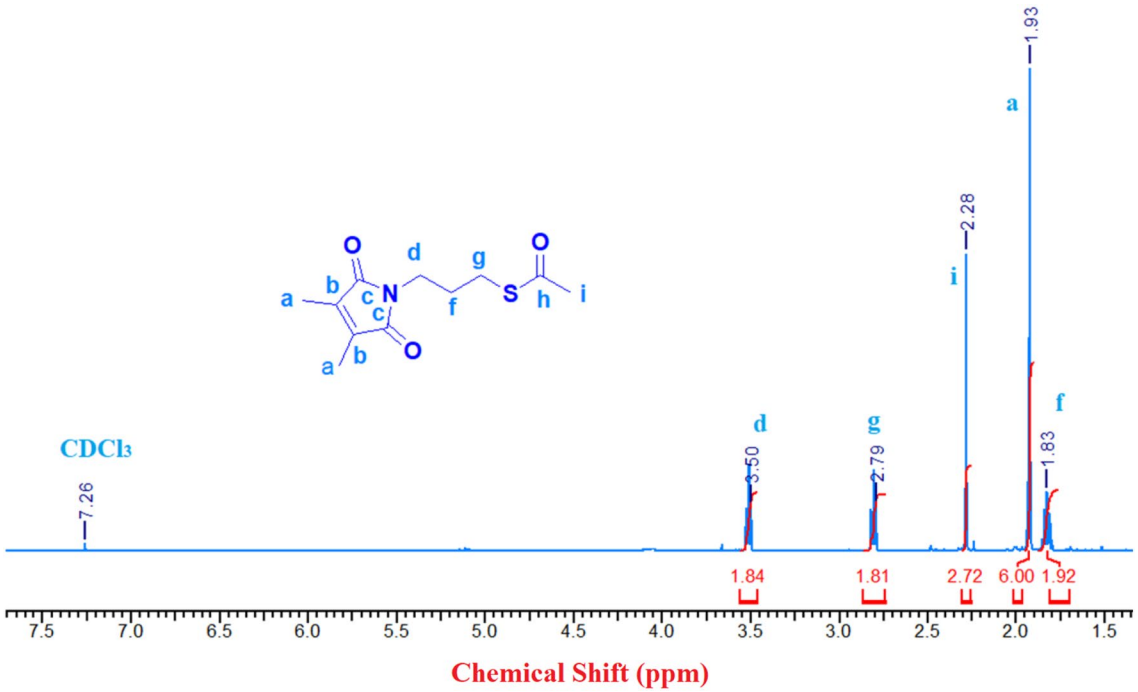

Fig. 6 1H NMR spectrum ($CDCl_3$) of thioacetic acid 3-(3, 4-dimethyl-2,5-dioxo-2,5-dihydro-pyrrol-yl)-propyl ester (DMITAc) (**6**)

(CH) at 3.74–4.13 ppm in a comparison with the integration of (2H) of (Ar-H) at 6.93–7.84 ppm; it was also observed the disappearance of vinyl monomers groups in the 1HNMR analysis proofing successful polymerization as shown in Fig. 7. All calculations were in a logic case with the feeding calculation Table 1. Furthermore, the FTIR of polymer recorded the presence of ester carbonyl group C=O at 1763 cm^{-1} and aldehyde carbonyl at 1713 cm^{-1} as represented in Fig. 8.

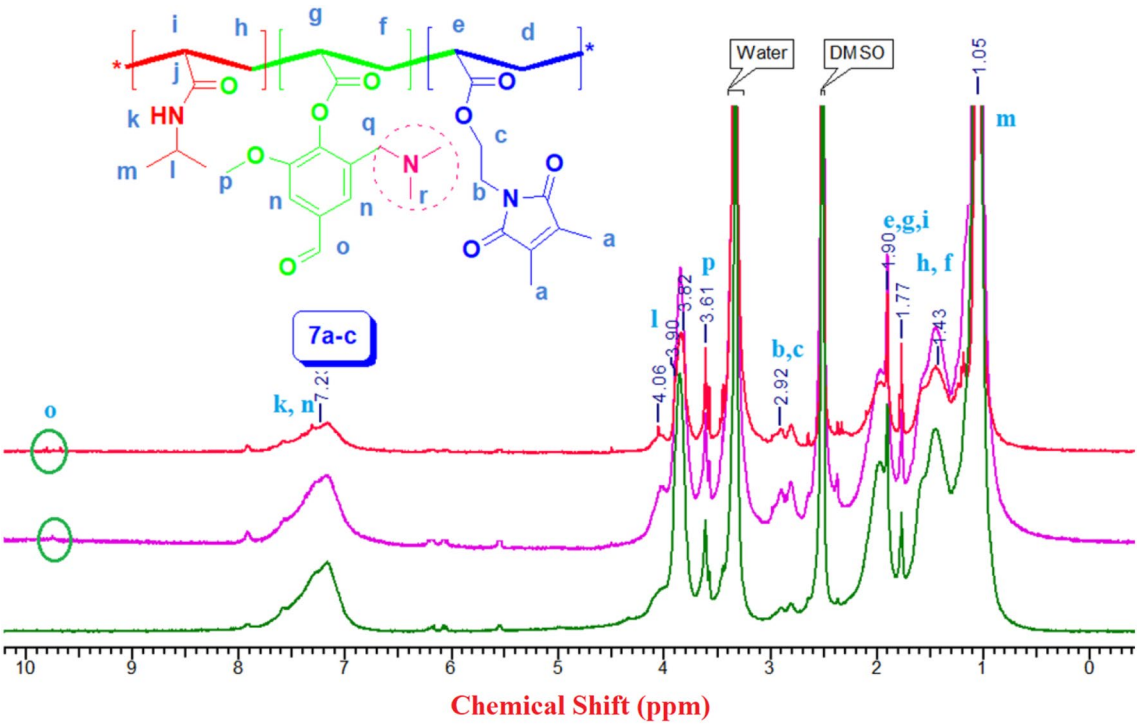

Fig. 7 1H NMR spectra ($CDCl_3$) of poly (NIPAAm-co-DMIA-co-DMAMVA)

Table 1 Yield, composition, weight average molecular weight, polydisperisity, glass temperature and lower critical solution temperature of P(NIPAAm-Co- DMIA-Co-DMAMVA)

Polymer	Yield (%)	Composition (mol%)		Mn^a (g/mol) 10^4	Đ[b]	T_g[c] (°C)	T_c[d] (°C) UV			T_c[d] (°C) SPR/OW hydrogel		
		[1]HNMR DMAMVA	UV DMIA				pH3	DI H_2O	pH12	pH3	DI H_2O	pH12
07–10	87	7.88	4.65	2.38	1.76	144.65	44.2	23	22.6	–	–	–
07–15	84	10.43	4.58	1.94	1.64	147.46	63.3	24.5	22	–	–	–
07–20	78	13.74	4.39	1.75	1.45	152.85	–	32.4	24.6	–	22.3	19.4

[a]Weight average molecular weight; [b]polydidperisty; [c]glass temperature; [d]lower critical solution temperature

Miscellaneous Properties of Polymers

Gel permeation chromatography (GPC) has been used to record the molecular weights (weight average molecular weight, number average molecular weight, and viscosity average molecular weight) as well as the dispersity of polymers **7a–c**. Polymers were dissolved in tetrahydrofuran (THF) and automated running. Figure 9 showed the GPC spectrum of polymer samples; it demonstrated an indirect relation between the molecular weight and dispersity with the molar concentration of vanillin acrylate monomer (DMAMVA) that might be attributed to the effect of the steric hindrances of monomers. Moreover, the spectrum for all polymers appeared as one peak with one height demonstrated the disappearance of low molecular weights molecules such as monomers and some other impurities. All data were summarized in Table 1.

The thermal properties of polymeric material have the greatest importance, which expresses the direction of material application. Differential scanning calorimeter (DSC) was used to measure the glass transition temperature (T_g) of photo-cross-linked polymers **7a–c** with a heating rate of 5℃/min, under a nitrogen atmosphere. The DSC spectra (diffractogram) as shown in Fig. 10; the recorded data exhibited direct relation between the molar concentrations of vanillin acrylate monomer (DMAMVA) and the glass temperatures *Tgs* values. It showed 144.65, 147.46, and 152.85 ℃ for 07–10, 07–15, and 07–20 respectively. The higher glass

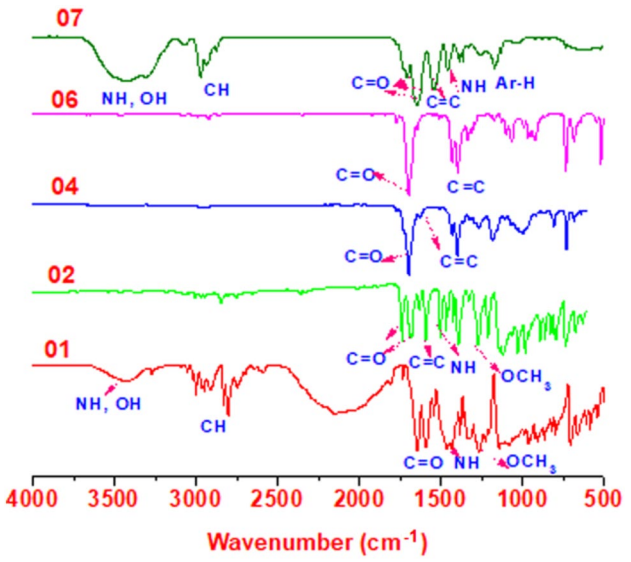

Fig. 8 FTIR of Monomer, photo-cross-linker, adhesion promotor and polymers

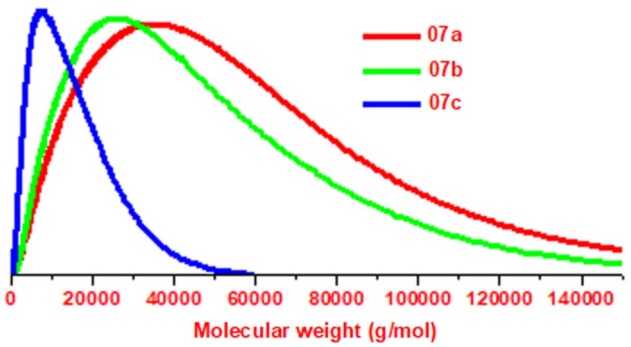

Fig. 9 GPC of polymers **07a–c**

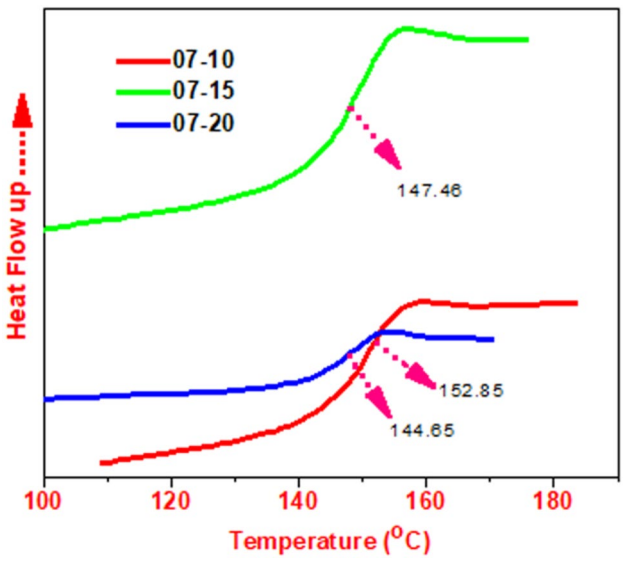

Fig. 10 DSC diffractogram for glass transition temperatures of polymers **07a–c**

temperature values of polymers than homo-PNIPAAm interpreted to the presence of tertiary amine group with aldehyde group that increased the hydrophilic characters of polymers and hence increased the glassy state and glass transition temperature as well. All recorded data were summarized in Table 1.

The Phase Separation and the Lower Critical Solution Temperature

The environmental or the smart behavior of the polymer solution to thermo-pH has been investigated and discussed in detail. The UV–VIS spectroscopy was used to measure the turbidity of polymer solution in deionized water, pH3, and pH12 as neutral, acidic, and basic media. The transmittance was recorded per 2 ℃ temperature scale. The relation of transmittance to temperature was drawn and the transition temperature was determined as the intersect point further, the temperature at 50% transmittance was known as the cloud point. The observations were pointed for three cases as follow:

Firstly, the transition temperature and the cloud point were investigated in the deionized water; the T_cs and C_ps values demonstrated 23, 24.5, and 32.4 ℃ corresponding to 25.5, 27, and 35.5 ℃ for 07–10, 07–15 and 07–20 respectively. An increase in the lower critical solution temperature and the cloud point as well by increasing the molar concentration of DMAMVA content in the polymer chain due to an increase in the hydrophilicity of polymer solution and increasing isotropic state rather than an anisotropic state. Secondly, the investigation has been done in pH3 referring to acidic media which effect dramatically in the polymeric solution and increased the ionization in the polymer solution. The protonation of the tertiary amine group has affected directly the lower critical solution temperature T_c and the cloud point C_p, it was observed much higher values of T_cs and C_ps 49.2 and 63.3 ℃ correspondings to 50.4 and 64 ℃ for polymers 07–10 and 07–15 respectively. For polymer 07–20 with 20 mol% of DMAMVA, we could not record any actual change in the transmittance by raising the temperature until 80 ℃, this fact can be interpreted as the higher T_c value than the maximum temperature was used by instrument. The last measurements of the lower solution temperature and cloud points were done in pH12. The turbidity has appeared at lower temperatures not only than measured in deionized water and pH3 but also more than measured for pure PNIPAAm in DI water. It demonstrated T_cs and C_ps at 22.6, 22 and 17.8 ℃ and 24.6, 23, and 20.2 for 07–10, 07–15, and 07–20, these attributed to the deactivation of hydrophilic

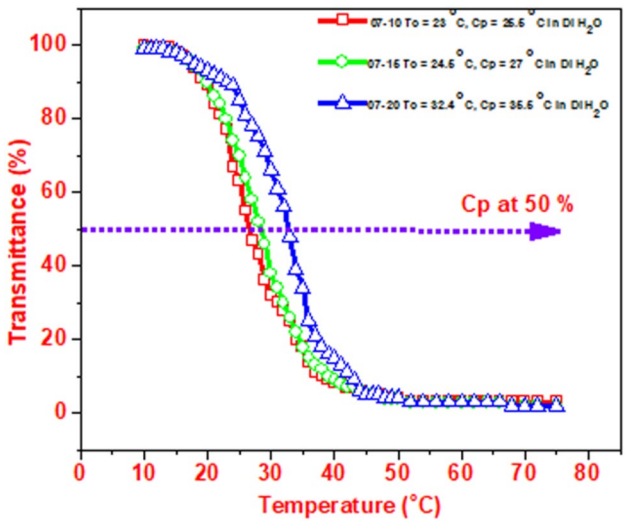

Fig. 11 The change in turbidity with temperature for LCST of P (NIPAAm-Co-DMAMVA-Co-DMIA) by UV–Vis spectroscopy for 1 wt% of polymer solution in deionized water

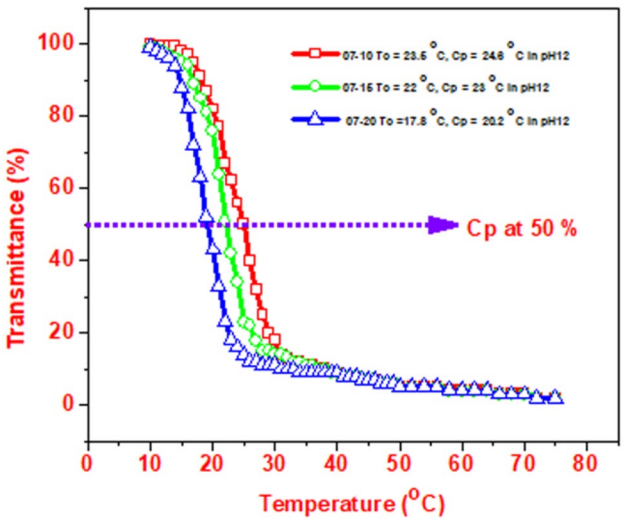

Fig. 13 The change in turbidity with temperature for LCST of P (NIPAAm-Co-DMAMVA-Co-DMIA) by UV–Vis spectroscopy for 1 wt% of polymer solution in pH12

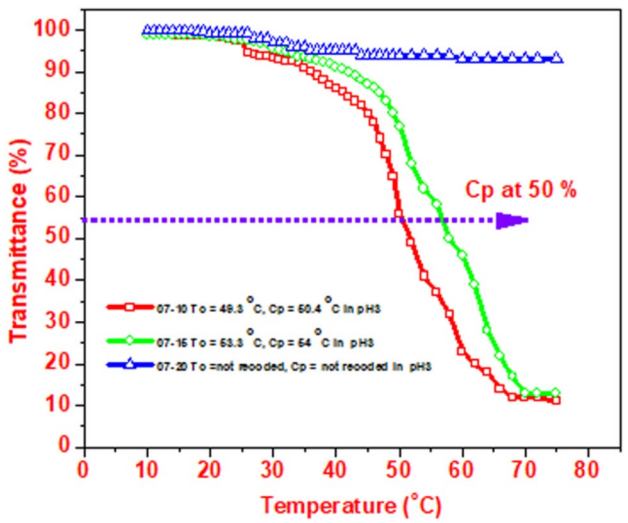

Fig. 12 The change in turbidity with temperature for LCST of P (NIPAAm-Co-DMAMVA-Co-DMIA) by UV–Vis spectroscopy for 1 wt% of polymer solution in pH3

groups and domination of hydrophobic one (Figs. 11, 12, 13).

Hydrogel Thin Films and SPR/OW for Swelling Properties and Transition Temperature

Previously, in the experimental part, we discussed the steps used for the formation of hydrogel thin films; these involved the deposition of the gold layer over LaSFN9 glass followed by immersing in DMITAc adhesion to form (LaSFN9 + Au + DMITAc adhesion). A solution of 7.5 wt% polymer 07–20 in distilled cyclohexanone was spin-coated and exposed to UV lamp for cross-linking. The thickness for each step was measured by SPR-OW spectroscopy according to Kretschmann configuration. The instrument allowed pathing Ne/He laser beam at 633 nm and penetrates the sample fixed with the prism. The incidence angle (θ) was varied with a goniometer and then pathed through a photodiode for collection. The reflected intensity versus angle was measured, and then Fresnel calculations were used to demonstrate the system of multi-layers [60–65]. Gold thin film was measured producing 46 nm thickness, and then with adhesion promoter was 52.41 nm as shown in Fig. 14. The dry film thickness was measured and calculated by Fresnel calculations resulted in 217.57 nm and refractive index 1.476 as clear in Table 2 and Fig. 15.

The pH-responsive properties of photo-cross-linked polymer hydrogel 07–20 were investigated as a function in the volume degree of swelling ($1/\chi_p$) and refractive index (n). Figure 16 illustrated the swelling as a change in RI (θ) with pH-dependent; it showed the highest plasmon minimum at ~64°. Fresnel simulations and calculations of volume degree of swelling and refractive index as a function of pH at 20 ℃ was done and demonstrated the highest the volume degree of swelling ($1/\chi_p$) and refractive index (n) at pH3 as the strongest acidic dielectric media that attributed to the high protonation and ionization of hydrogel, as shown in Fig. 17.

The lower critical solution temperature and the phase separation of the photo-cross-linked polymer hydrogel 07–20 were determined as a function in pH dielectric media. The first running has been done in deionized water; the reflection intensity RI (θ) as a change in temperature was scanned and demonstrated the highest value of

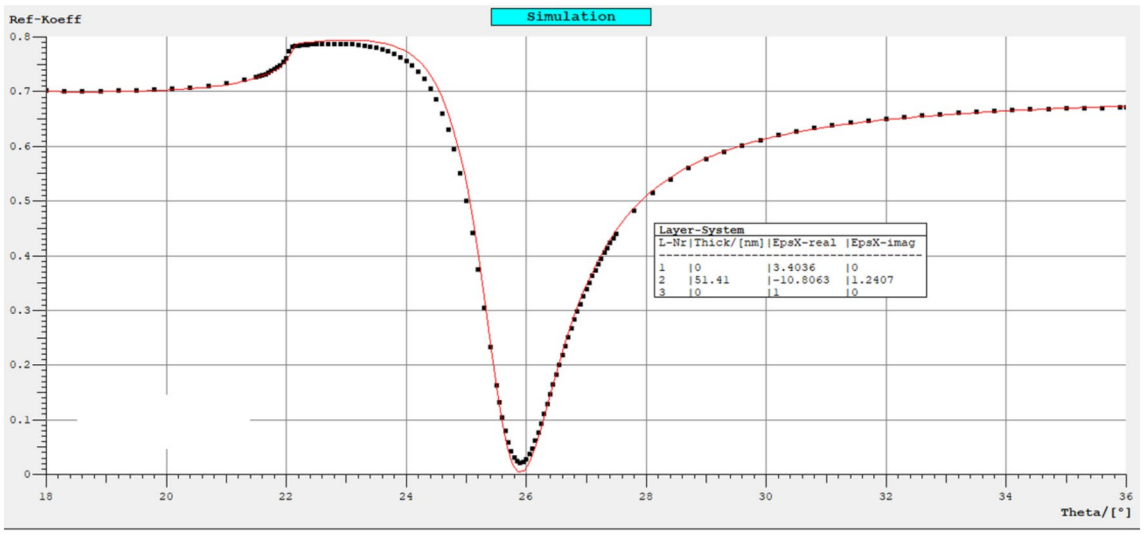

Fig. 14 SPR scan of photo-cross-liked hydrogel layer RI (θ) as experimentally (black line) and simulation (red line) and Fresnel calculations in the model box for the (Au + adhesion promotor) (Color figure online)

Table 2 The Fresnel calculations of dry hydrogel layers system for thickness, dielectric and refractive index

Polymer	Dry thickness	Dielectric ($n^2 = \varepsilon$)	$n = \sqrt{\varepsilon}$
07–20	217.57	2.18	1.476

reflected angle at the dry state, while, the lowest value was observed at the top of swelling state as shown in Figs. 18 and 19. The volume degree of swelling and refractive index versus temperature was used to determine the T_c of the hydrogel at the onset point exhibited at 22.3 ℃. With the same method, the lower critical solution temperature was determined in pH12 and pH3; in the strongest basic dielectric media pH12, it showed T_c at 19.4 ℃ Fig. 20, while it did not respond at pH3 attributed to the expected transition temperature is higher than the maximum temperature used by the instrument, Fig. 21.

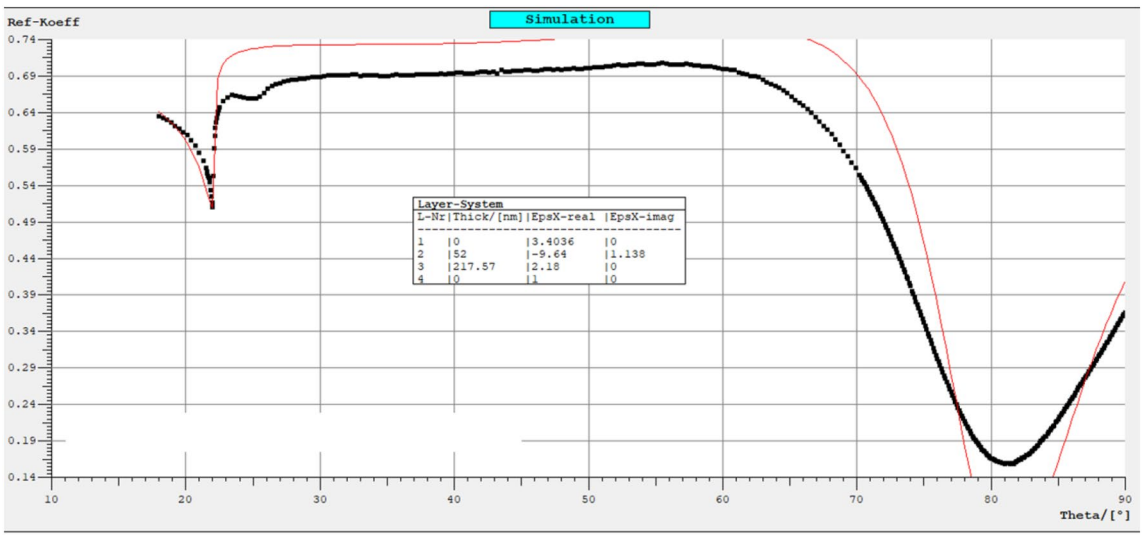

Fig. 15 SPR scan of photo-cross-liked hydrogel layer RI (θ) as experimentally (black line) and simulation (red line) and Fresnel calculations in the model box for the dry film thickness **(07–20)** (Color figure online)

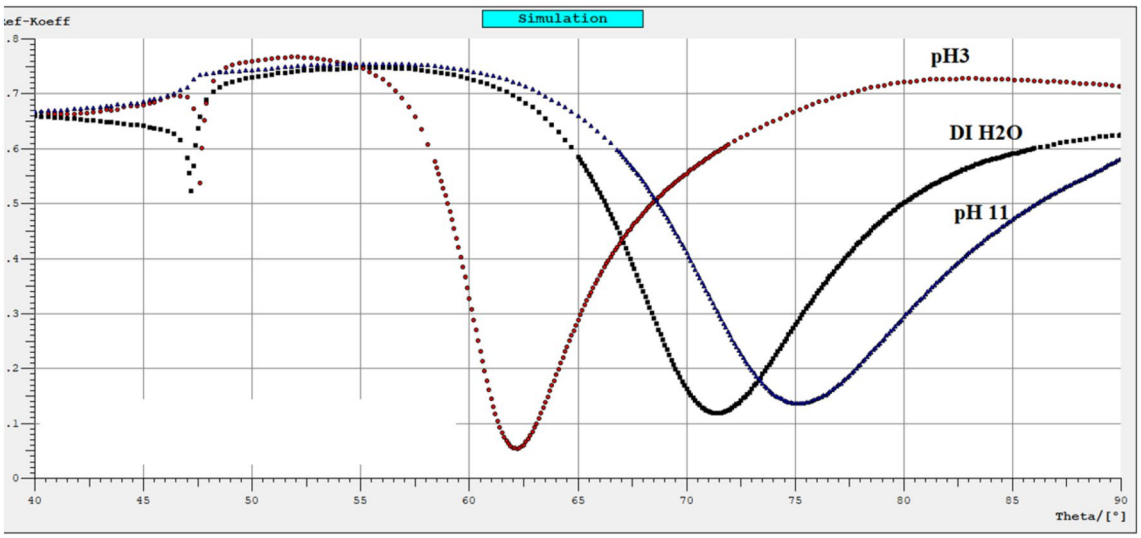

Fig. 16 SPR scan of photo-cross-linked hydrogel layer RI (θ) with pH variations of bilayer **(07–20)**

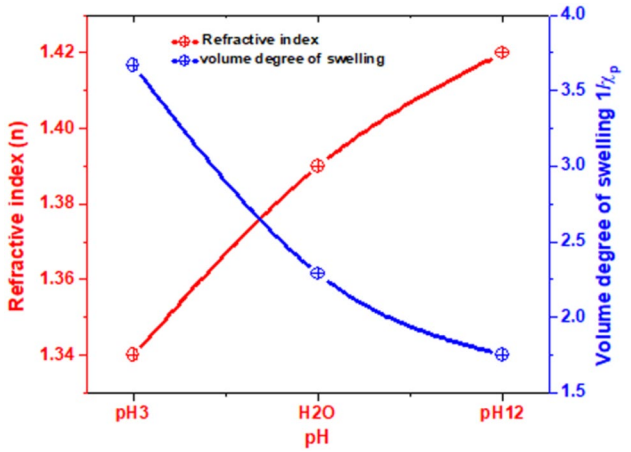

Fig. 17 The volume degree of swelling and refractive index vs. pH of photo-cross-linked hydrogel layer for **(07–20)**

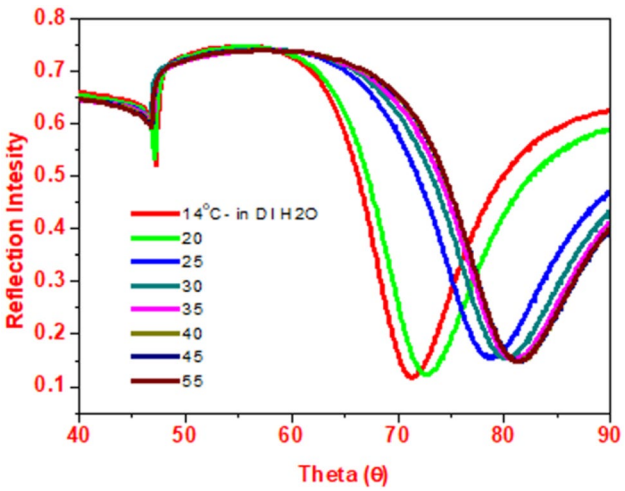

Fig. 18 SPR scan of photo-cross-linked hydrogel layer RI (θ) with pH variations of bilayer **(07–20)**

Conclusion

The present study emphasizes the preparation of dually thermos-pH photo-cross-linked polymers based on N-isopropylacrylamide, and the new monomer has synthesized from vanillin and acted as a pH-responsive monomer in the polymer chains. Three different photo-cross-linker polymers with the different molar concentrations of DMAMVA have been fabricated; they exhibited an effective in the general characterizations of polymers. They demonstrated different lower critical solution temperatures at different ambient environments, in DI water, polymer solution showed lower values of T_c that increased by increasing the concentration of DMAMVA, the same results have been demonstrated for T_c at pH12. The highest values of T_c were observed at pH3 as the ionization of the amino group and the effect of electrostatic attraction between the solution and polymer chain was activated. The next step was focused on the formation of dual-responsive hydrogel thin films as layer by layer. The hydrogel layer thin films have been successfully built, and the thickness was determined by the SPR-OW technique according to the simulation of Kretschmann configuration. The volume degrees of swelling and refractive indexes have been calculated and they were used in the determination of phase separation temperature that showed closed value to the polymer solution. In the nearest future, the photo-cross-linked polymer will be used for the formation of bilayer hydrogel thin films as

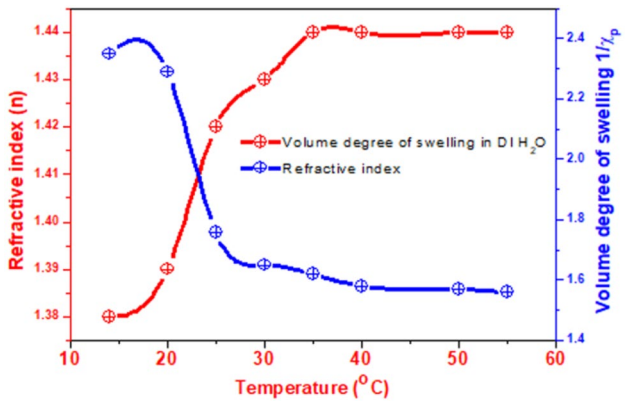

Fig. 19 The volume degree of swelling and refractive index vs. temperature of photo-cross-linked hydrogel layer in DI H_2O

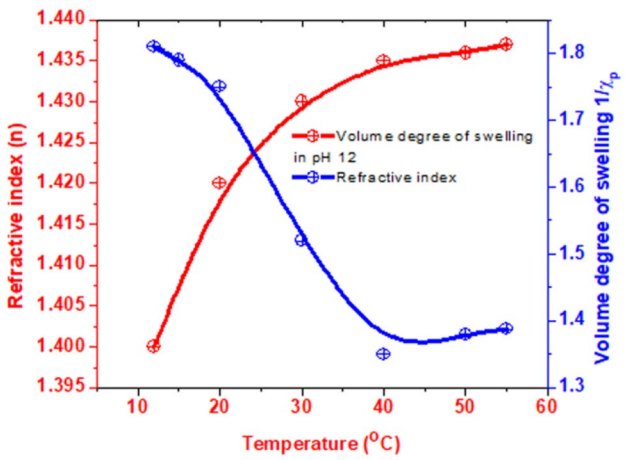

Fig. 20 The volume degree of swelling and refractive index vs. temperature of photo-cross-linked hydrogel layer in pH12

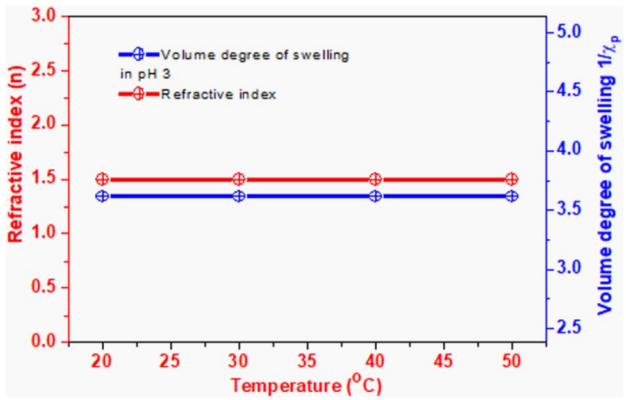

Fig. 21 The volume degree of swelling and refractive index vs. temperature of photo-cross-linked hydrogel layer in pH3

responsive and non-responsive for biocompatible vessel technology.

Acknowledgements The author is gratefully acknowledged to Egyptian culture and missions, and The Deutscher Akademischer Austauch (DAAD) for financial assistance during the post-doctor work in Germany of Momen S.A. Abdelaty.

Compliance with Ethical Standards

Conflict of interest The author declares no conflict of interest.

References

1. Seidi F, Jenjob R, Crespy D (2018) Designing smart polymer conjugates for controlled release of payloads. Chem Rev 11:3965–4036. https://doi.org/10.1021/acs.chemrev.8b00006
2. Liang H, Qiang Z, Xue L, Michael JS (2019) Stimuli-responsive polymers for sensing and actuation. Mater Horiz 6:1774–1793. https://doi.org/10.1039/C9MH00490D
3. Xiaoming H, Chen Z, Yufu T, Feng L, Yuanyuan L, Feng P, Xiaomei L, Yu J, Jie L, Wenjun W, Quli F, Wei H (2019) Intelligent polymer–MnO_2 nanoparticles for dual-activatable photoacoustic and magnetic resonance bimodal imaging in living mice. Chem Commun 55:6006–6009. https://doi.org/10.1039/C9CC02148E
4. Abdelaty MSA (2018) Poly(N-isopropylacrylamide-co-2-((diethylamino)methyl)-4 formyl-6-methoxyphenylacrylate) environmental functional copolymers: synthesis, characterizations, and grafting with amino acids. Biomolecules 8:138. https://doi.org/10.3390/biom8040138
5. Abdelaty MSA (2018) Preparation and characterization of new environmental functional polymers based on vanillin and N-isopropylacrylamide for post polymerization. J Polym Environ 26:636–646. https://doi.org/10.1007/s10924-017-0960-2
6. Chen J-K, Chang C-J (2014) Fabrication and applications of stimuli-responsive polymer films and patterns on surface. Materials 7:805–875. https://doi.org/10.3390/ma7020805
7. Richard H (2014) Temperature-responsive polymers: properties, synthesis, and applications. Smart Polym Appl. https://doi.org/10.1016/B978-0-08-102416-4.00002-8
8. Kocak G, Tuncer C, Bütün V (2017) pH-responsive polymers. Polym Chem 8:144–176. https://doi.org/10.1039/C6PY01872F
9. Tao X, Ting L, Wei-Feng Z, Cheng-Sheng Z (2019) Ionic-strength responsive Zwitterionic copolymer hydrogels with tunable swelling and adsorption behaviors. Langmuir 35(5):1146–1155
10. Shohei I, Miki M, Hironobu K, Yoshitsugu H, Shokyoku K (2019) Swelling and mechanical properties of thermoresponsive/hydrophilic conetworks with crosslinked domain structures prepared from various triblock precursors. Polym Chem 10:6122–6130. https://doi.org/10.1039/C9PY01417A
11. Valentina M, Pierfrancesco C, Marta G, Bartosz T, Veronica A (2017) Light-responsive polymer micro- and nano-capsules. Polymers 9:1–19. https://doi.org/10.3390/polym9010008
12. Abdelaty MSA, Kuckling D (2016) Synthesis and characterization of new functional photo cross-linkable smart polymers containing vanillin derivatives. Gels 2:76. https://doi.org/10.3390/gels2010003
13. Jayakumar A, Jose KV, Lee J-M (2020) Hydrogels for medical and environmental applications. Small Methods. https://doi.org/10.1002/smtd.201900735

14. Junsoo K, Solyee I, Jeong HK, Sang MK, Seung-Min L, Jaewoo L, Jong P, Jiyong W, Seung EM (2020) Thermoresponsive hydrogels: artificial perspiration membrane by programmed deformation of thermoresponsive hydrogels. Adv Mater. https://doi.org/10.1002/adma.202070039
15. Klouda L, Mikos AG (2008) Thermoresponsive hydrogels in biomedical applications—a review. Eur J Pharm Biopharm 68:34–45. https://doi.org/10.1016/j.ejpb.2007.02.025
16. Ajji Z, Maarouf M, Khattab A, Ghazal H (2020) Synthesis of pH-responsive hydrogel based on PVP grafted with crotonic acid for controlled drug delivery. Radiat Phys Chem 170:108612. https://doi.org/10.1016/j.radphyschem.2019.108612
17. Angus RH, Pradeep K, Yahya EC, Pierre PDK, Thashree M, Lisa CT, Viness P (2017) Design of a versatile pH-responsive hydrogel for potential oral delivery of gastric-sensitive bioactives. Polymers 9:474. https://doi.org/10.3390/polym910047
18. Liang X, Linzi Q, Yang S, Yixin S, Linhong D, Xinqing L, Mark B, Rong Z (2018) Biodegradable pH-responsive hydrogels for controlled dual-drug release. J Mater Chem B 6:510–517. https://doi.org/10.1039/C7TB01851G
19. Jamali A, Moghbeli MR, Ameli F, Roayaie E, Karambeigi MS (2020) Synthesis and characterization of pH-sensitive poly(acrylamide-co-methylenebisacrylamide-co-acrylic acid) hydrogel microspheres containing silica nanoparticles: application in enhanced oil recovery processes. J Appl Polym Sci 137:48491. https://doi.org/10.1002/app.48491
20. Ankita B, Judy MA-B, Anthony G-E (2020) Toward impedimetric measurement of acidosis with a pH-responsive hydrogel sensor. ACS Sensors. https://doi.org/10.1021/acssensors.9b02336
21. Shibayama M, Tanaka T (1993) Volume phase transition and related phenomena of polymer gels. Adv Polym Sci 109:1–62. https://doi.org/10.1007/3-540-56791-7-1
22. Costa E, Coelho M, Ilharco LM, Aguiar-Ricardo A, Hammond PT (2011) Tannic acid mediated suppression of PNIPAAm microgels thermoresponsive behaviour. Macromolecules 44:612–621. https://doi.org/10.1021/ma1025016
23. Andrew C, Kyoung DS, Hyungjun Y, Seon JH, Dong SK (2019) Bulk poly(N-isopropylacrylamide) (PNIPAAm) thermoresponsive cell culture platform: toward a new horizon in cell sheet engineering. Biomater Sci 7:2277–2287. https://doi.org/10.1039/C8BM01664J
24. Abdul Haq M, Su Y, Wang D (2017) Mechanical properties of PNIPAM based hydrogels: a review. Mater Sci Eng C 70:842–855. https://doi.org/10.1016/j.msec.2016.09.081
25. Abdelaty MSA (2019) Influence of vanillin acrylate and 4 acetylphenyl acrylate hydrophobic functional monomers on phase separation of N isopropylacrylamide environmental terpolymer: fabrication and characterization. Polym Bull. https://doi.org/10.1007/s00289-019-02890-0
26. Maria VM, Maria M, Cesar AB (2018) Poly(N-isopropylacrylamide) Crosslinked gels as intrinsic amphiphilic materials. swelling properties used to build novel interphases. J Phys Chem B 122:9038–9048
27. Akhilesh KG, Nicholas AP, Ali K (2014) Nanocomposite hydrogels for biomedical applications. Biotechnol Bioeng 111:441–453. https://doi.org/10.1002/bit.25160
28. Javad T, Youhong T (2017) Hydrogel based sensors for biomedical applications: an updated review. Polymers 9:364. https://doi.org/10.3390/polym9080364
29. Yang HW, Chena JK, Cheng CC, Kuo SW (2013) Association of poly(N-isopropylacrylamide) containing nucleobase multiple hydrogen bonding of adenine for DNA recognition. Appl Surf Sci 271:60–69. https://doi.org/10.1016/j.apsusc.2013.01.074
30. Jabbari E, Tavakoli J, Sarvestani AS (2007) Swelling characteristics of acrylic acid polyelectrolyte hydrogel in a dc electric field. Smart Mater Struct 16:1614
31. Kocak G, Tuncera C, Bütün V (2017) pH-Responsive polymers. Polym Chem 8:144–176. https://doi.org/10.1039/C6PY01872F
32. Thomas S, Linda S, Mark G, Stephen R (2016) The pH-responsive behaviour of poly(acrylic acid) in aqueous solution is dependent on molar mass. Soft Matter 12:2542. https://doi.org/10.1039/c5sm02693h
33. Abdelaty MSA (2018) Preparation and characterization of environmental functional poly(styrene-Co-2-[(diethylamino) methyl]-4-formyl-6-methoxy-phenyl acrylate) copolymers for amino acid post polymerization. Open J Polym Chem 8:41–55. https://doi.org/10.4236/ojpchem.2018.83005
34. Liu M, Ishid Y, Ebina Y, Sasaki T, Hikima T, Takata M, Aida T (2015) An anisotropic hydrogel with electrostatic repulsion between cofacially aligned nanosheets. Nature 517:68–72. https://doi.org/10.1038/nature14060
35. Umit G, Oguz O (2014) Self-healing poly(acrylic acid) hydrogels with shape memory behavior of high mechanical strength. Macromolecules 47(19):6889–6899. https://doi.org/10.1021/ma5015116
36. Sean B, Dyer N, Anthony G-E (2003) Release characteristics of novel pH-sensitive p(HEMA-DMAEMA) hydrogels containing 3-(trimethoxy-silyl) propyl Methacrylate. Biomacromol 4(5):1224–1231
37. Tavakoli J, Tang Y (2017) Honey/PVA hybrid wound dressings with controlled release of antibiotics: Structural, physico-mechanical and in vitro biomedical studies. Mater Sci Eng 77:318–325
38. Han L, Lu X, Wang M, Gan D, Deng W, Wang K, Fang L, Liu K, Chan CW, Tang Y et al (2017) A mussel-inspired conductive, self-adhesive, and self-healable tough hydrogel as cell stimulators and implantable bioelectronics. Small 13:1000. https://doi.org/10.1002/smll.201601916
39. Ertürk G, Mattiasson B (2017) Molecular imprinting techniques used for the preparation of biosensors. Sensors 17:288
40. Abdelaty, M.S.A., and Kuckling D. (2018) Poly (N-Isopropyl Acrylamide-Co-Vanillin Acrylate) Dual Responsive Functional Copolymers for Grafting Biomolecules by Schiff's Base Click Reaction. Open Journal of Organic Polymer Materials. 8,15-32. 10.4236/ojopm.2018.82002
41. Caygill RL, Blair GE, Millner PA (2010) A review on viral biosensors to detect human pathogens. Anal Chim Acta 681:8–15
42. Castillo J, Gaspar S, Leth S, Niculescu M, Mortari A, Bontidean I, Soukharev V, Someanu SA, Ryabov AD, Csoregi E (2004) Biosensors for life quality: design, development and applications. Sensors Actuators B 102:179–194
43. Han Z, Wang P, Mao G, Yin T, Zhong D, Yiming B, Hu X, Jia Z, Nian G, Qu S, Yang W (2020) A dual pH-responsive hydrogel actuator for lipophilic drug delivery. ACS Appl Mater Interfaces. https://doi.org/10.1021/acsami.9b21713
44. Chen D, Liu H, Kobayashib T, Yu H (2010) Multiresponsive reversible gels based on a carboxylic azo polymer. J Mater Chem 20:3610–3614. https://doi.org/10.1039/B925163D
45. Pasparakisa G, Vamvakaki M (2011) Multiresponsive polymers: nano-sized assemblies, stimuli-sensitive gels and smart surfaces. Polym Chem 2:1234–1248
46. Yajie L, Chaocan Z, Youliang Z, Yixiao D, Wanyu C (2015) Novel multi-responsive polymer materials: when ionic liquids step in. Euro Polym J 69:441–448. https://doi.org/10.1016/j.europolymj.2015.05.023
47. Sebastian H, Torsten R, Hendrik B, Sebastian S (2014) Multiresponsive polymer hydrogels by orthogonal supramolecular chain cross-linking. Macromolecules 47(12):4028–4036. https://doi.org/10.1021/ma5008573
48. Hossein H, Soleyman H, Shahryar P, Naser G, Rohollah M (2019) Synthesis of multiresponsive β-cyclodextrin nanocomposite through surface RAFT polymerization for controlled

drug delivery. Polym Adv Technol 30:2860–2871. https://doi.org/10.1002/pat.4718
49. Ramkissoon-Ganorkar C, Baudys M, Wan Kim S (2000) Effect of ionic strength on the loading efficiency" of the model polypeptide/protein drugs in pH-/temperature-sensitive polymers. J Biomater Sci Polym Ed 11:45–54
50. Ju HK, Kim SY, Kim SJ, Lee YM (2002) pH/temperature-responsive semi-IPN hydrogels composed of alginate and poly(N-isopropylacrylamide). J Appl Polym Sci 11:28–1139. https://doi.org/10.1002/app.10137
51. Li X, Sun Q, Li Q, Kawazoe N, Chen G (2018) Functional hydrogels with tunable structures and properties for tissue engineering applications. Front Chem 6:499. https://doi.org/10.3389/fchem.2018.00499
52. Debroy D, Li-Oakey KD, Oakey J (2019) Engineering functional hydrogel microparticle interfaces by controlled oxygen-inhibited photopolymerization. Colloids Surf B Biointerfaces 180:371–375. https://doi.org/10.1016/j.colsurfb.2019.05.001
53. Huang R, Kostanski LK, Filipe CDM, Ghosh R (2009) Environment-responsive hydrogel-based ultrafiltration membranes for protein bioseparation. J Membr Sci 336:42–49. https://doi.org/10.1016/j.memsci.2009.03.002
54. Zhen L, Zhijun X, Liuyin F, Hua X, Chengxi C (2017) An ionic coordination hybrid hydrogel for bioseparation. Chem Commun 53:5842–5845. https://doi.org/10.1039/C7CC01923H
55. Rakchoy S, Suppakul P, Jinkarn T (2009) Antimicrobial effectsof vanillin coated solution for coating paper board intended for packaging bakery products. Asian J Food Agroindustry 2:138–147
56. Imanishi H, Sasaki YF, Matsumoto K (1990) Suppression of 6-TG-resistant mutations in V79 cells and recessive spot formations in mice by vanillin. Mutat Res Lett 243:151–158
57. Ho K, Yazan LS, Ismail N, Ismail M (2009) Apoptosis and cell cycle arrest of human colorectal cancer cell line HT-29 induced by vanillin. Cancer Epidemiol 20:155–160
58. Acik G (2020) Bio-based Poly(ε-caprolactone) from soybean-oil derived polyol via ring-opening polymerization. J Polym Environ 28:668–675. https://doi.org/10.1007/s10924-019-01597-7
59. Acik G, Karatavuk AO (2020) Synthesis, properties and biodegradability of cross-linked amphiphilic poly(vinyl acrylate)-poly(tert-butyl acrylate)s by photo-initiated radical polymerization. Eur Polym J 127: Article 109618. https://doi.org/10.1016/j.eurpolymj.2020.109602
60. Samuel SH, Kristy SM, Quan C (2018) Surface plasmon resonance: material and interface design for universal accessibility. Anal Chem 90(1):19–39. https://doi.org/10.1021/acs.analchem.7b04251
61. Amendola V, Pilot R, Frasconi M, Maragò OM, Iatì MA (2017) Surface plasmon resonance in gold nanoparticles: a review. J Phys Condens Matter 29:203002. https://doi.org/10.1088/1361-648X/aa60f3
62. Abdelaty MSA (2018) Environmental functional photo-cross-linked hydrogel bilayer thin films from vanillin (part 2): temperature responsive layer A, functional, temperature and pH layer B. Polym Bull 11:4837–4858. https://doi.org/10.1007/s00289-018-2297-y
63. Abdelaty MSA (2019) Layer by layer photo-cross-linked environmental functional hydrogel thin films based on vanillin: part 3. J Polym Environ. https://doi.org/10.1007/s10924-019-01421-2
64. Nan Zhang N, Knoll W (2009) Thermally responsive hydrogel films studied by surface plasmon diffraction. Anal Chem 81:2611–2617. https://doi.org/10.1021/ac802527j
65. Anac I, Aulasevich A, Junk MJN, Jakubowicz P, Roskamp RF, Menges B, Jonas U, Knoll W (2010) Optical characterization of co-nonsolvency effects in thin responsive PNIPAAm-based gel layers exposed to ethanol/water mixtures. Macromol Chem Phys 211:1018–1025. https://doi.org/10.1002/macp.200900533
66. Kuckling D, Hoffmann J, PlÖtner M, Ferse D, Kretschmer K, Adler H-JP, Arndt K-F, Reichelt R (2003) Photo cross-linkable poly(N-isopropylacrylamide) copolymers III: micro-fabricated temperature responsive hydrogels. Polymer 44:4455–4462. https://doi.org/10.1016/S0032-3861(03)00413-0
67. Harmon ME, Kuckling D, Pareek P, Frank CW (2003) Photo-cross-linkable PNIPAAm copolymers. 4. Effects of copolymerization and cross-linking on the volume-phase transition in constrained hydrogel layers. Langmuir 19:10947–10956. https://doi.org/10.1021/la030217h